Crustal structure at the western end of the North Anatolian Fault Zone from deep seismic sounding

Ali E. Karahan, Hans Berckhemer and Bodo Baier
Institute of Meteorology and Geophysics, University of Frankfurt am Main, Germany

Abstract
The first deep seismic sounding experiment in Northwestern Anatolia was carried out in October 1991 as part of the «German - Turkish Project on Earthquake Prediction Research» in the Mudurnu area of the North Anatolian Fault Zone. The experiment was a joint enterprise by the Institute of Meteorology and Geophysics of Frankfurt University, the Earthquake Research Institute (ERI) in Ankara, and the Turkish Oil Company (TPAO). Two orthogonal profiles, each 120 km in length with a crossing point near Akyazi, were covered in succession by 30 short period tape recording seismograph stations with 2 km station spacing. 12 shots, with charge sizes between 100 and 250 kg, were fired and 342 seismograms out of 360 were used for evaluation. By coincidence an $M_L = 4.5$ earthquake located below Imroz Island was also recorded and provided additional information on Moho and the sub-Moho velocity. A ray tracing method orginally developed by Weber (1986) was used for travel time inversion. From a compilation of all data two generalized crustal models were derived, one with velocity gradients within the layers and one with constant layer velocities. The latter consists of a sediment cover of about 2 km with $V_p \approx 3.6$ km/s, an upper crystalline crust down to 13 km with $V_p \approx 5.9$ km/s, a middle crust down to 25 km depth with $V_p \approx 6.5$ km/s, a lower crust down to 39 km Moho depth with $V_p \approx 7.0$ km/s and $V_p \approx 8.05$ km/s below the Moho. The structure of the individual profiles differs slightly. The thickest sediment cover is reached in the Izmit-Sapanca-trough and in the Akyazi basin. Of particular interest is a step of about 4 km in the lower crust near Lake Sapanca and probably an even larger one in the Moho (derived from the Imroz earthquake data). After the catastrophic earthquake of Izmit on 17 August 1999 this significant heterogeneity in crustal structure appears in a new light with regard to the possible cause of the Izmit earthquake. Heterogeneities in structure are frequently also heterogeneities in strength and stress that impede or even lock rupture. The Izmit earthquake is discussed in relation to a large *stepover* or *jog* at the North Anatolian Fault.

Key words *North Anatolian Fault Zone – crustal structure – deep seismic sounding*

1. Introduction

The North Anatolian Fault Zone is one of the most active parts of the Alpine-Mediterranean-Himalayan seismic belt. A joint German - Turkish research project was launched in 1985 to study the seismicity and different kinds of earthquake related phenomena in the Mudurnu valley area of the Northwestern Anatolian Fault Zone in view of earthquake prediction research. A network of 12 short period seismograph stations was installed and operated jointly by the Institute of Meteorology and Geophysics of Frankfurt University and the Earthquake Research Institute (ERI) in Ankara, to monitor the seismicity and, in particular, to locate the hypocenters in the test area. No specific crustal model for the seismic velocities was available for the area. Instead a model derived from refraction seismic data in Eastern Greece was used.

Mailing address: Prof. Hans Berckhemer, Institut für Meteorologie und Geophysik, Universität Frankfurt, Feldbergstraße 47, D-60323 Frankfurt am Main, Germany; e-mail: berckhem@geophysik.uni-frankfurt.de

Some incomplete information from quarry blasts near Adapazari (Gürbüz *et al.*, 1980) and near Anadolu Kavagi, Bosporus (Küleli *et al.*, 1996), observed mainly at a few permanent seismograph stations, gave a rough indication of crustal thickness and P_n velocity. Using earthquake observations from the MARNET network Gürbüz *et al.* (1991) inferred a Moho depth between 27 km near Istanbul and 34 km in the Marmara area. In 1987, a 300 km long north-south running reflection seismic traverse was carried out in cooperation with Turkish Petrol Inc. (TPAO) and the Turkish Research Institute for Science and Technology (TÜBITAK) with the aim of studying the crustal structure in Central Anatolia. A Moho depth of about 36 km was deduced from two-way-reflection-times of 12 s for the northern part of the profile.

In order to obtain a reliable seismic crustal model for the Mudurnu test area, a Deep Seismic Sounding (DSS) survey using reversed and orthogonal seismic profiles was planned and

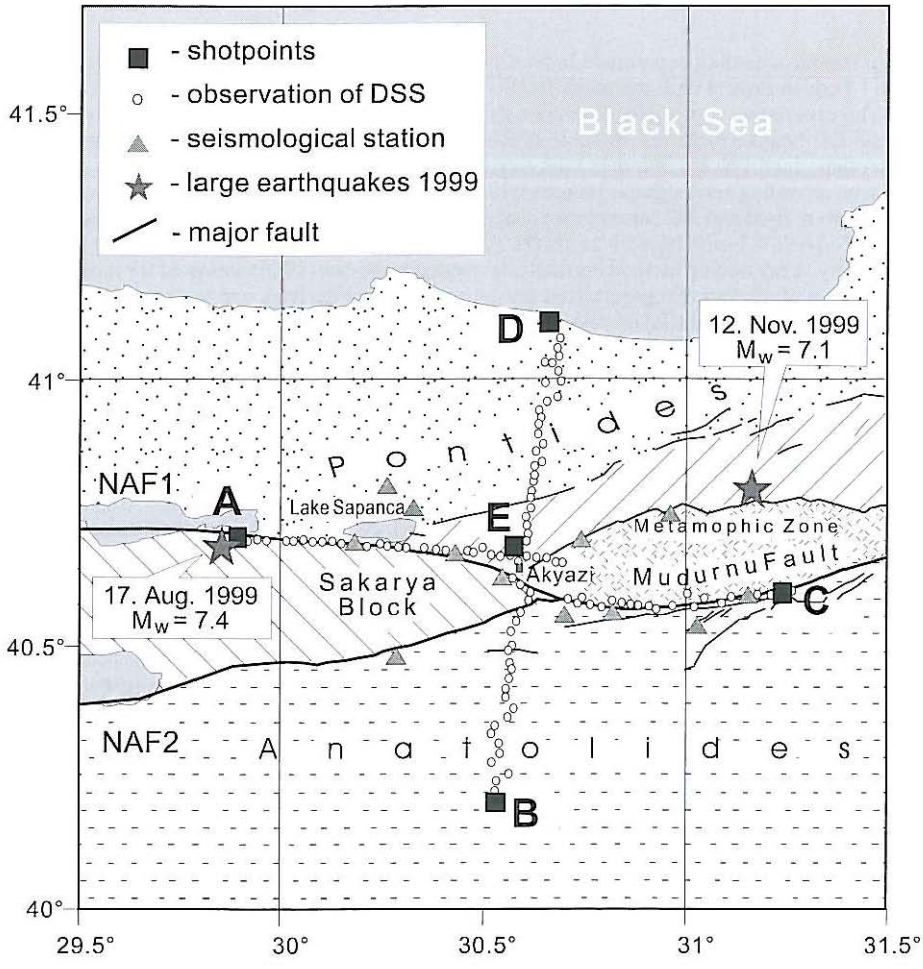

Fig. 1. Map of the area under investigation (modified after Neugebauer *et al.*, 1997), position of deep seismic sounding profiles, and large earthquakes in 1999.

performed in October 1991. This was the first true deep seismic sounding experiment carried out in Western Anatolia.

2. Geological description of the test area and the execution of the experiments

The North Anatolian Fault (NAF) represents, with the Pontides in the north and the Anatolian block in the south, a major boundary element of the Eurasian plate and the Arabian plate. The total right lateral displacement of the western NAF is estimated to be 85 km since the Middle Miocene (Sengör *et al.*, 1985; Dewey *et al.*, 1986). West of the Holocene basin of Adapazari-Akyazi the NAF forks into a west trending branch NAF1 and a southwest trending branch NAF2 (fig. 1).

Two profiles of about 120 km length were covered with 60 recording stations each. The W-E Profile followed closely the northern branch of the NAF from shotpoint A at the Gulf of Izmit, to shotpoint C near Lake Abant. The N-S Profile, from shotpoint D in the delta of the river Sakarya at the Black Sea coast in the north to shotpoint B near Yenipazar in the south, crossed the W-E Profile at right angles in the Adapazari basin. Here, at E, four additional shots were fired. Individual charges of 25 kg each were emplaced in 4 inch drill holes of 30-50 m depth. The total charge size of each blast ranged from 100 to 250 kg and is listed in table I. Permission from the authorities could only be obtained for charge sizes up to 250 kg, thus a desirable extension of the profiles beyond 120 km was unrealistic.

Recording of the seismic signals was carried out with 30 units of magnetic tape recording seismographs (type MLR) developed in the Institute of Meteorology and Geophysics, Frankfurt University. Sixty kilometers of profile length were covered by one set up of stations, with a spacing of 2 km. A unit consisted of a 1 Hz vertical component seismometer with 3 level recording of the amplitude modulated signal using a tape speed of 0.33 mm/s which allows a continuous recording time of 3 weeks. This had the advantage that the instruments could be left unattended and blasting could be carried out at any suitable time, preferably at night. The radio time signal from the long wave transmitter station DCF (near Frankfurt/Germany) was record-

Table I. List of shots.

Profile section	Shot	Date	Time (MET)	Charge size (kg)
A-E	A1	10.10.1991	05:11:46.24	100
E-C	A2	16.10.1991	19:35:03.25	200
E-D	B1	21.10.1991	19:00:02.84	250
B-E	B2	24.10.1991	18:59:59.95	150
E-A	C1	13.10.1991	19:00:03.00	200
C-E	C2	17.10.1991	19:00:03.38	100
D-E	D1	20.10.1991	19:00:19.29	150
E-B	D2	25.10.1991	19:00:01.12	250
E-A	E1	11.10.1991	19:00:29.52	100
E-C	E2	17.10.1991	04:10:03.46	100
E-D	E3	20.10.1991	22:23:25.06	150
E-B	E4	25.10.1991	22:00:01.61	150

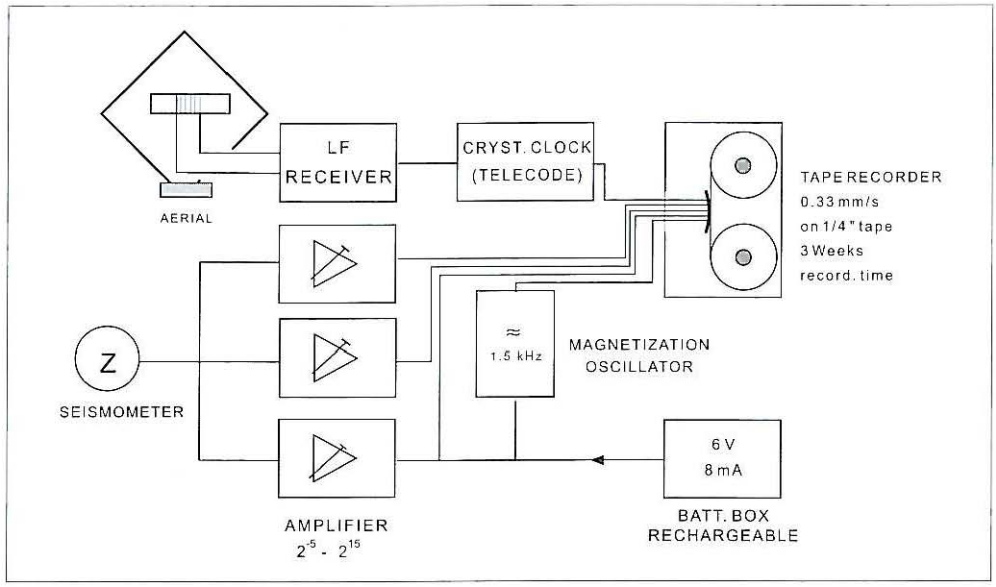

Fig. 2. Mobile Long term seismic Recording system (MLR).

ed on the fourth channel (fig. 2). It may be mentioned that recording systems of the same type were also used at the permanent stations of the Mudurnu seismograph network (see fig 1). Some of these were 3-component stations.

Playback of the tapes was performed on a four channel digital transient-recorder. The digitized data were processed (normalization of amplitudes, frequency filtering for the optimum signal/noise ratio, static corrections for altitude of station and source).

3. Data

For complete documentation of the data all seismogram sections are presented in the upper part of figs. 3a-h. The position of the profiles is shown on fig. 1. Travel times are reduced by 6.0 km/s. The reference altitudes to which the travel times have been reduced are given in the figure captions. Onsets or changes in signal shape have been picked visually and, to indicate likely correlations, marked by common symbols such as circles, squares, diamonds, stars or crosses. The correlations shown below the seismogram sections in figs. 3a-h have subsequently been used in the travel time inversion and interpretation of the seismograms. A total of 360 seismograms was obtained during the experiment, of which 324 could be used for evaluation. With the exception of Shot C1 (Profile C-A, 60-120 km) the seismic energy of the different phases was rather good. Details of the uppermost sedimentary layer could only be roughly resolved with the station spacing of about 2 km. As mentioned above, due to the limited profile length, P_n-first arrivals could not be observed and the information on Moho depth is largely based on wide angle reflections P_MP at overcritical distances. These arrivals were particularly well developed at Shot B1 (fig. 3g).

Fortunately the Imroz Earthquake of October 12, 1991 was recorded on Profile Section A-E and at about 20 permanent seismograph stations (see fig. 6) of the region which allowed a fairly accurate determination of the P_n velocity.

The shots with date, time, and charge size are listed in table I.

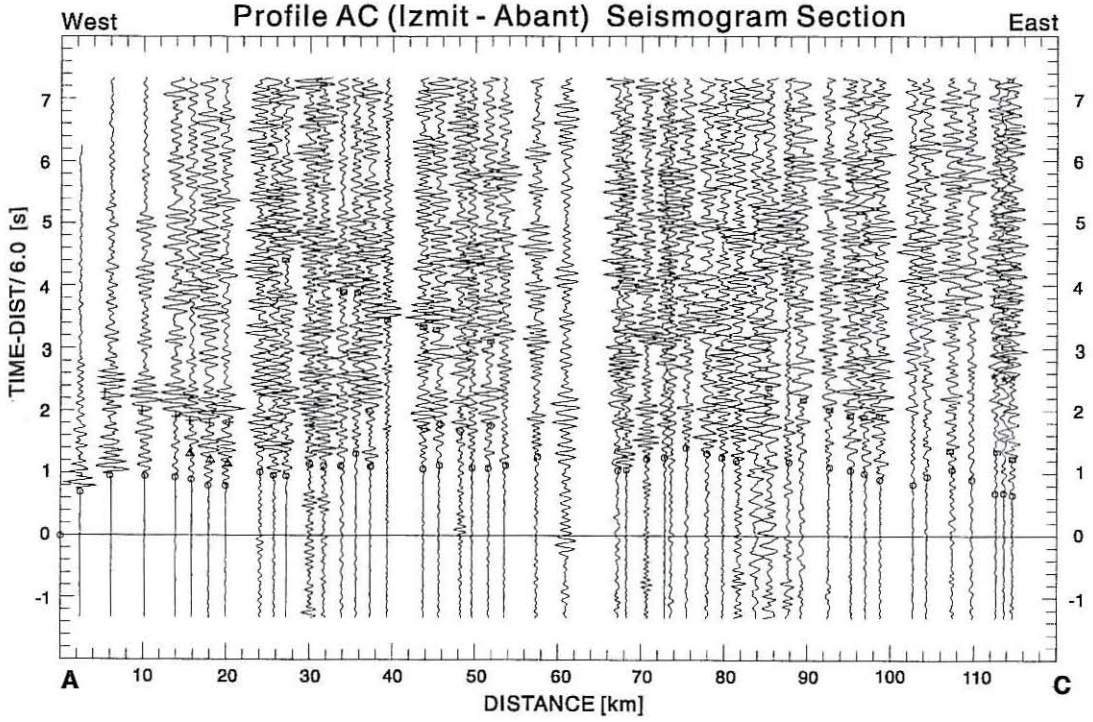

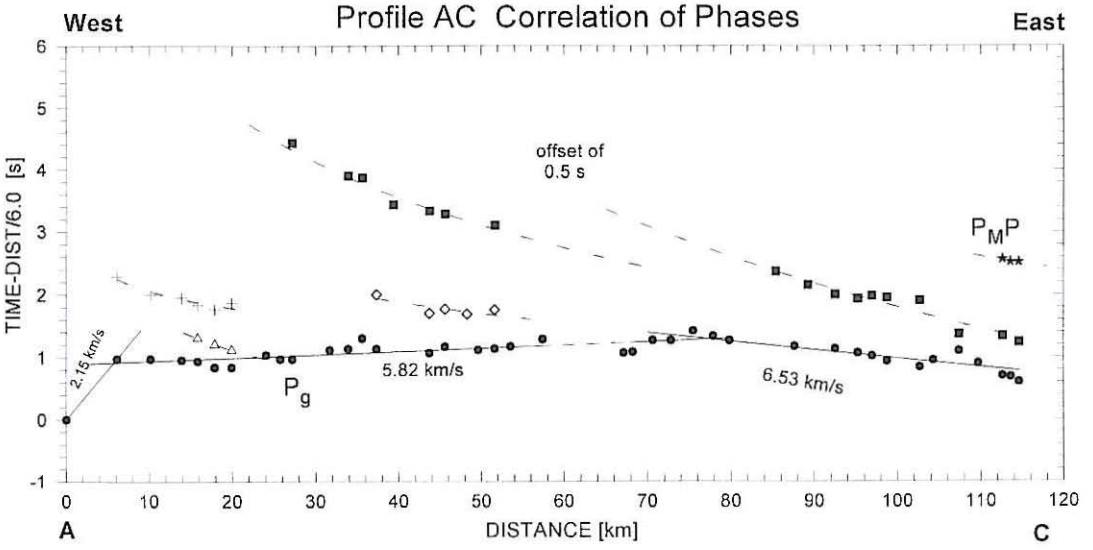

Fig. 3a. Seismogram Section AC, Shotpoint A (reference level 100 m NN). Below: correlations of phases used for interpretation. Solid lines are used for first arrivals with usually good signal/noise ratio, dashed lines are used for correlation of later arrivals, sometimes with lower signal /noise ratio.

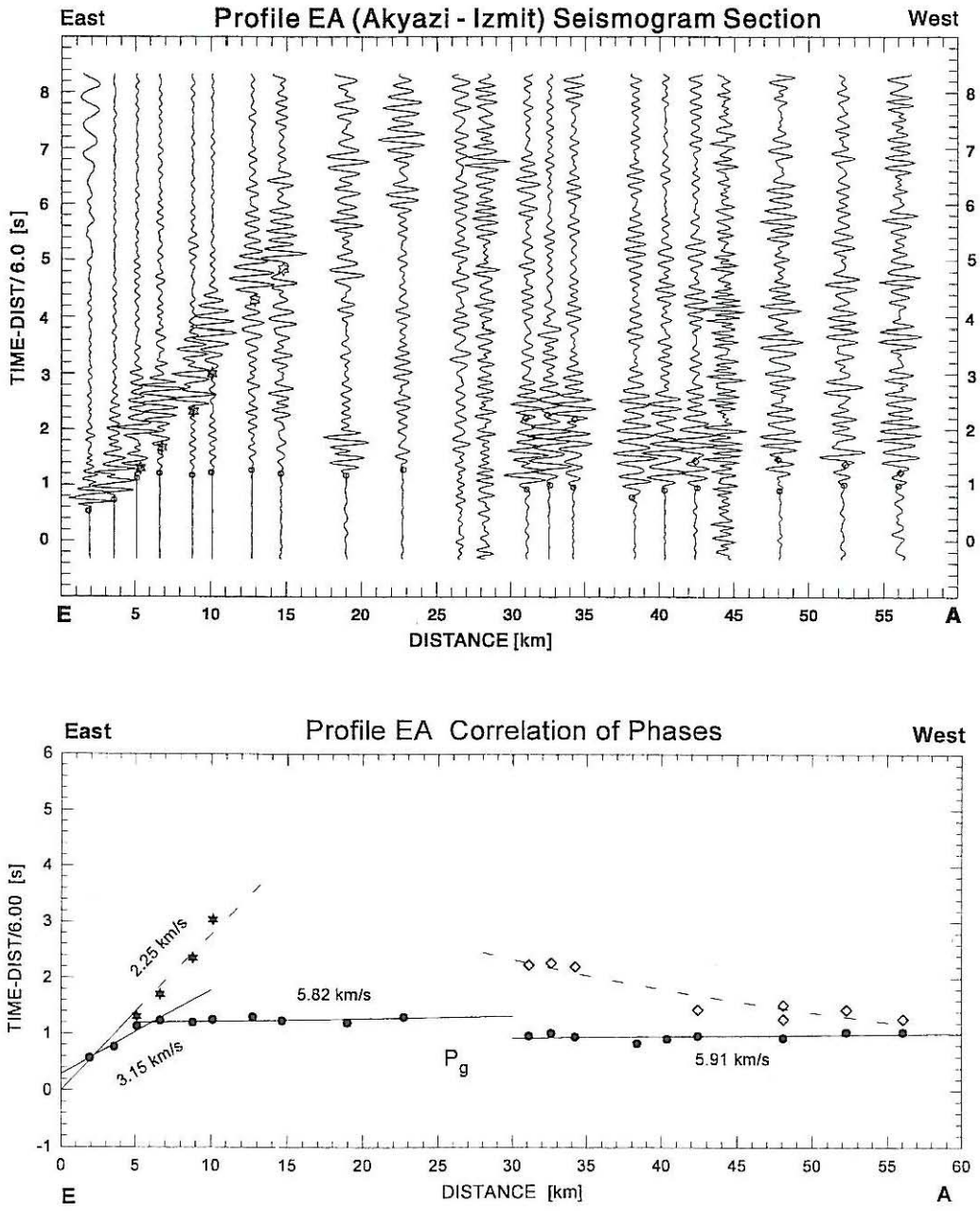

Fig. 3b. Seismogram Section EA, Shotpoint E (reference level 100 m NN). Below: correlation of phases used for interpretation.

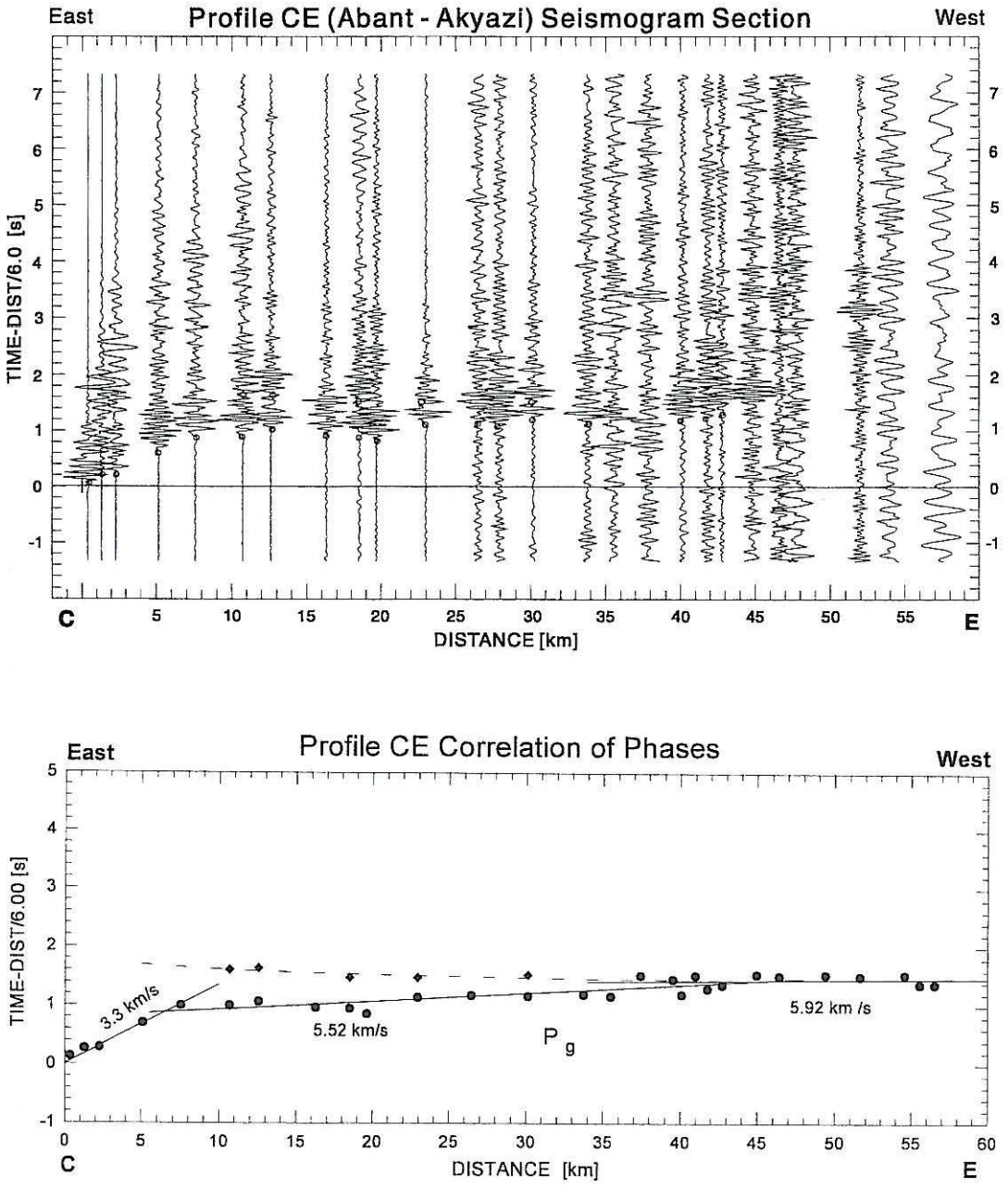

Fig. 3c. Seismogram Section CE, Shotpoint C (reference level 1400 m NN). Below: correlations of phases used for interpretation.

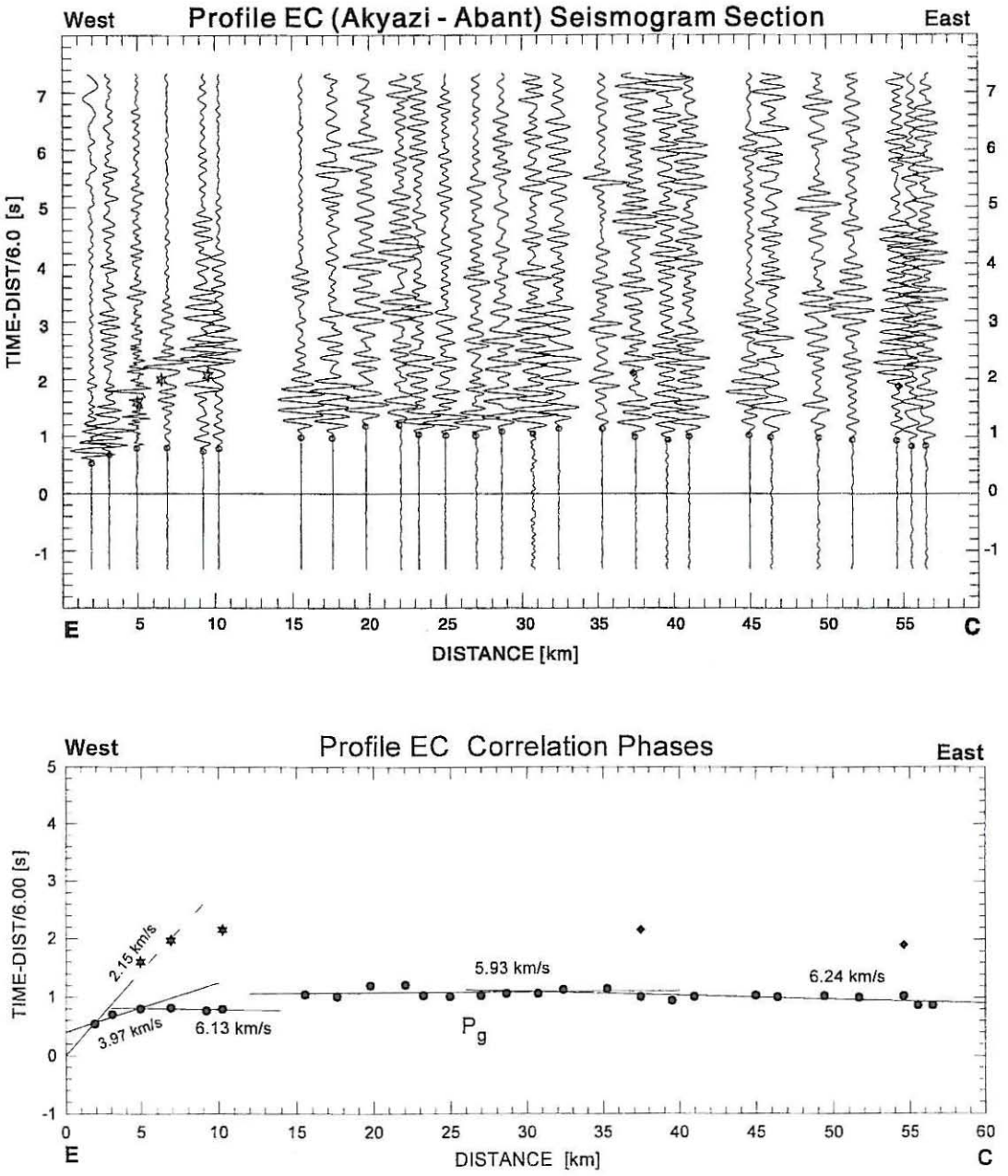

Fig. 3d. Seismogram Section EC, Shotpoint E (reference level 100 m NN). Below: correlation of phases used for interpretation.

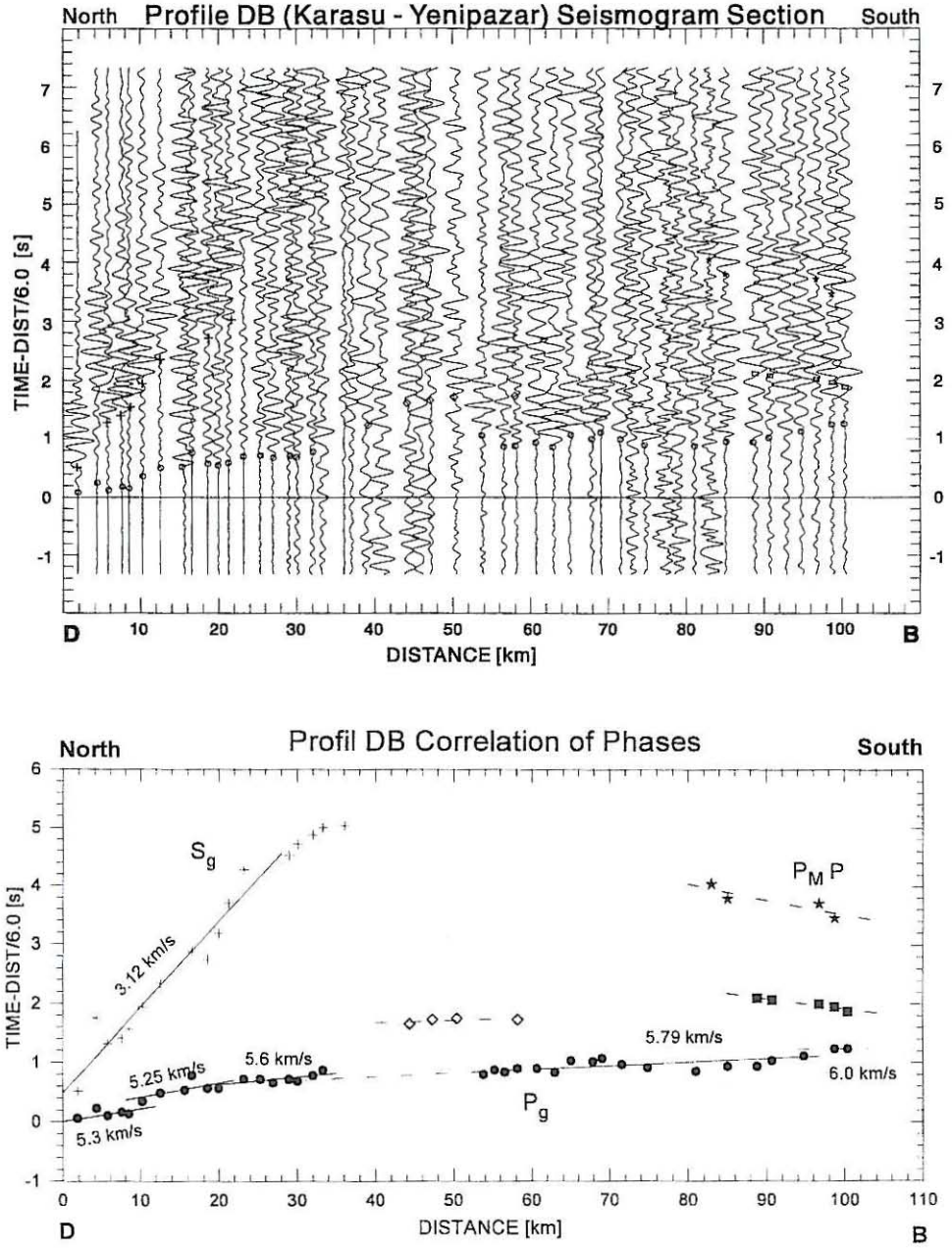

Fig. 3e. Seismogram Section DB, Shotpoint D (reference level 100 m NN). Below: correlation of phases used for interpretation.

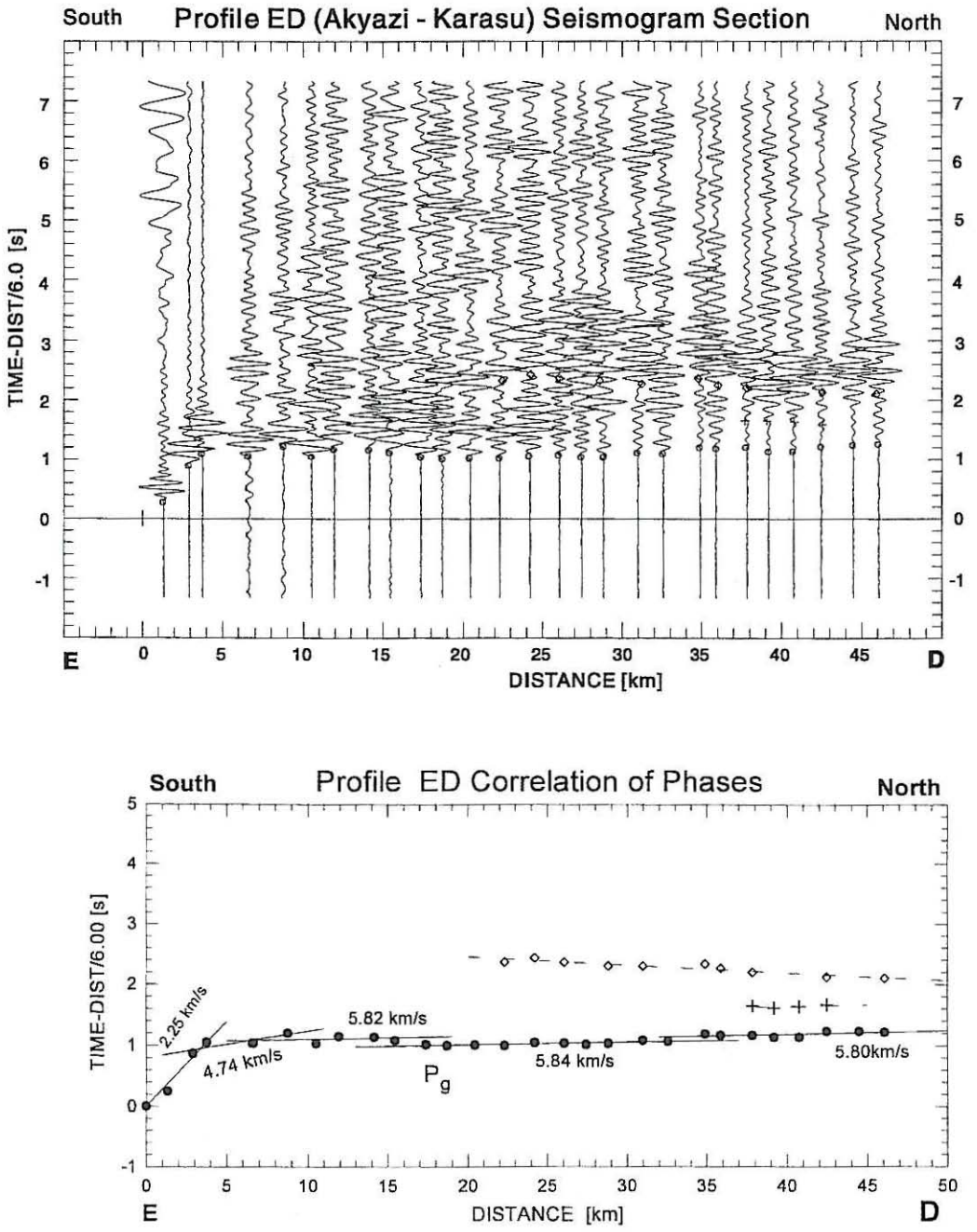

Fig. 3f. Seismogram Section ED, Shotpoint E (reference level 100 m NN). Below: correlation of phases used for interpretation.

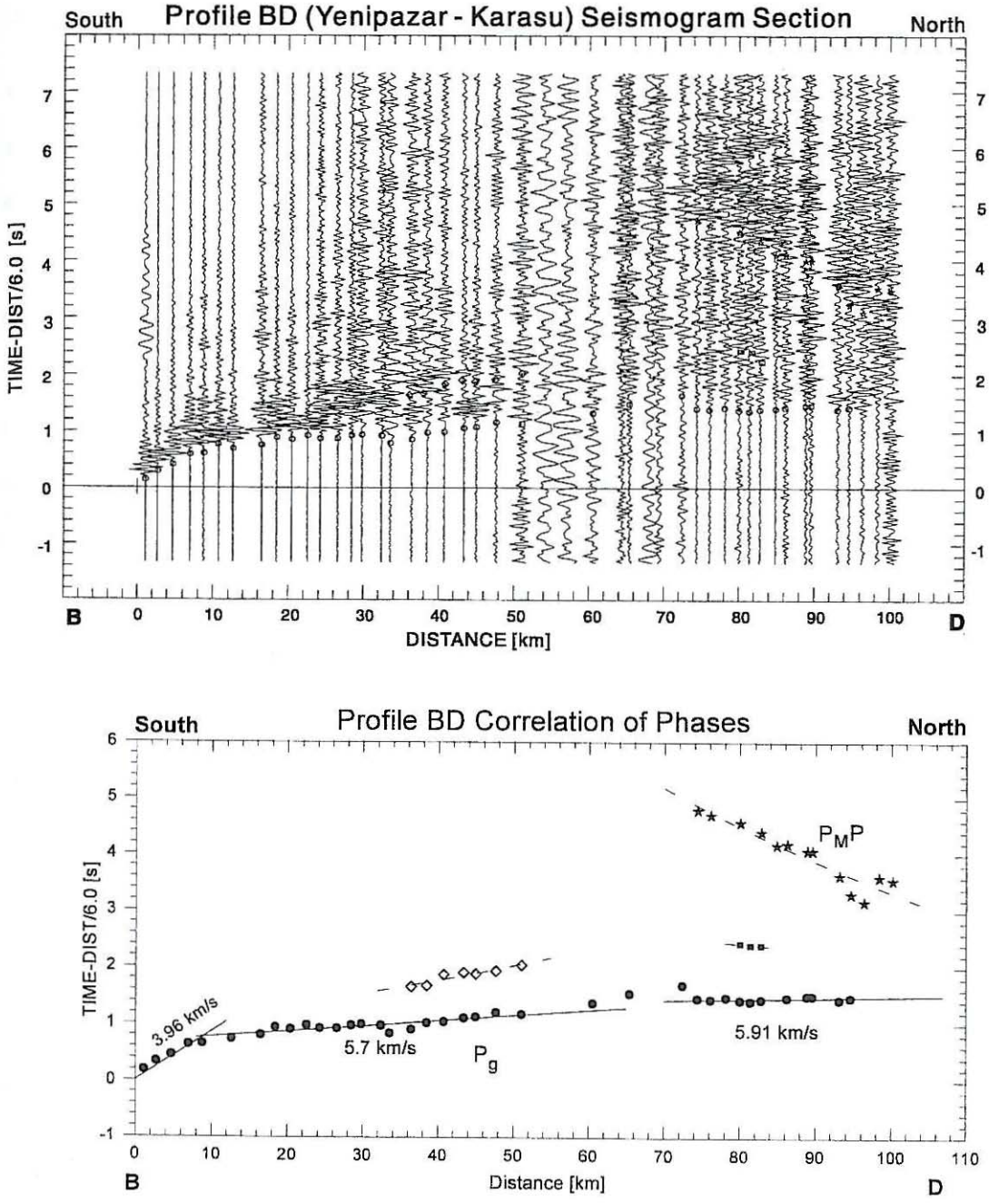

Fig. 3g. Seismogram Section BD, Shotpoint B (reference level 700 m NN). Below: correlation of phases used for interpretation.

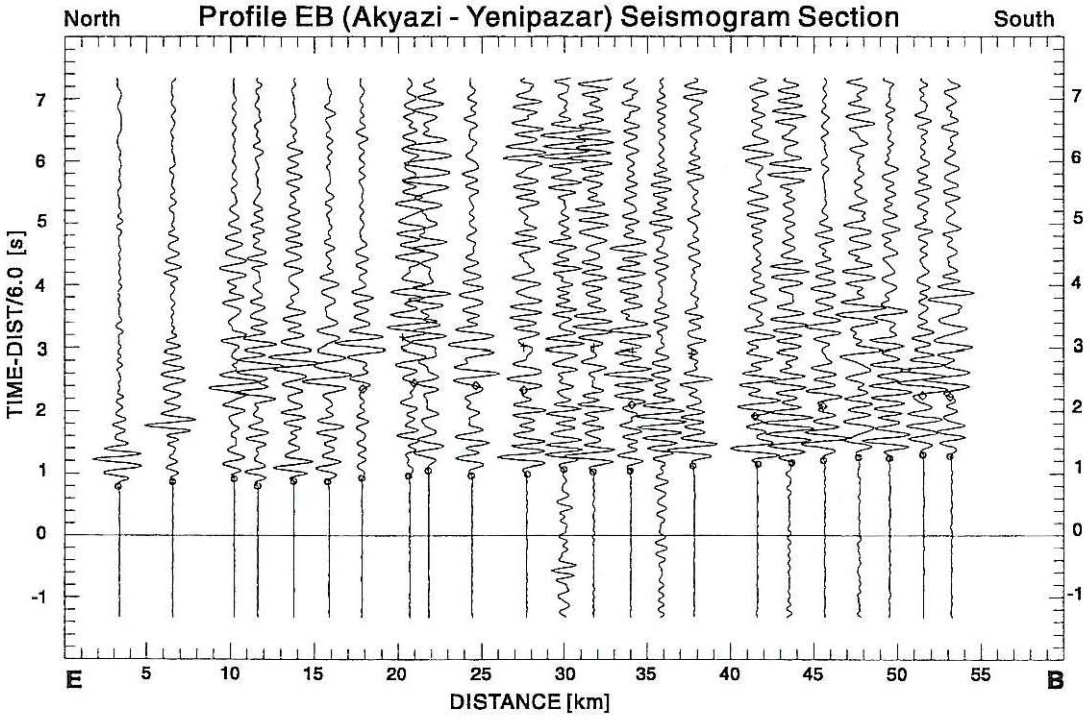

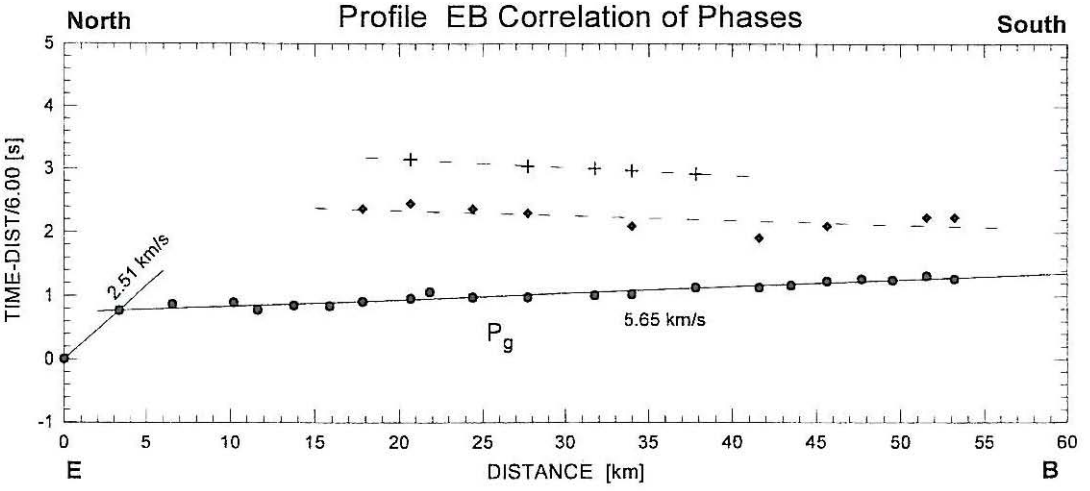

Fig. 3h. Seismogram Section EB, Shotpoint E (reference level 100 m NN). Below: correlation of phases used also in crustal section fig. 5.

4. Travel time inversion of seismograms

Experience shows that certain basic features can be found in all travel time diagrams of crustal deep seismic soundings. We usually observe for weakly increasing velocity with depth P_g at shorter distances and P_n at sufficiently large distances as first arrivals. In terms of the ray concept, these are normal branches of the travel time graphs, which mean, that with decreasing angle of incidence of the ray, the distance of emergence increases and the travel time curve has (in principle) a convex curvature. P_g comes from the crystalline basement, P_n from the uppermost mantle (critical refracted wave). Rays from wide angle reflections at discontinuities, or diving waves from zones with strong velocity gradients, form reverse branches in the travel time plot where, with decreasing angle of incidence, the distance of emergence decreases and the curvature of the travel time curve is concave. This is, in particular, the case at the transition from crust to mantle (P_MP), which is of importance in the present case, where the P_n-distance could not be reached. Reverse travel time branches originate also from velocity boundaries within the crust.

4.1. *Inversion methods used*

Classical direct inversion methods for plane interfaces allow the derivation of a first order approximation velocity – depth structure and have been used to obtain starting models for more sophisticated indirect numerical data inversion. In the present study a two-dimensional ray tracing method was used which is part of a software package for the Gauss Beam Method developed by Weber (1986) and adapted for PCs by Schulze-Frerichs (1988).

This program allows us to handle refracted, reflected and converted waves. Complex 2-dimensional geological structures can be modelled by dividing the medium into triangles with linear velocity laws. The model input is defined by parametrisation of the corners of the triangles in terms of P (and S) velocity values. Nodes common to several triangles may have different velocity values for the different space elements. In this way, the free surface, and first and second order discontinuities can be modelled. For more details of the method see Weber (1986) and Karahan (1998).

Computations of synthetic seismograms, attempted in a few cases, have not significantly improved the travel time inversion results and are therefore not presented here.

5. Presentation and interpretation of profiles

A considerable number of ray tracing models for the individual seismogram sections have been computed and compared with the correlated arrivals (for details see Karahan ,1998), Here only *one* complete crustal section is shown for the W-E Profile (fig. 4) and *one* for the S-N Profile (fig. 5), but some conclusions presented below are based on additional raytracing models not shown explicitly in this paper.

5.1. *W-E Profile (Izmit-Abant)*

Shotpoint A (fig. 3a) – The first arrivals at short distances from A can be interpreted as those from unconsolidated sediments with V_p of 2.15 km/s. At a depth of only 1.8 km the crystalline basement, with a velocity of 5.8-5.9 km/s, is reached. Between distances of 4 and 20 km, later arrivals with remarkably large amplitudes, marked by crosses in the correlation below, follow the first arrivals with a delay time of about 2 s. These are interpreted as side wall reflections from the Sakarya-basement block, south of the profile. P_g can be traced up to distances of 80 km where it is overtaken by a branch with $V_p \approx 6.5$ km/s. Noticeable are two branches of later arrivals (black squares) at distances of 20-55 km and 80-115 km with a time offset of about 0.5 s between them. These represent wide angle reflections from a boundary between 22.3 and 26.5 km in depth. The offset can best be interpreted as a step of about 4 km in the lower crust. This is the result of several raytracing tests described in detail by Karahan (1998). Figure 4 shows a ray tracing model including this feature. Whether this step exists also in the depth of the Moho cannot be decided from the DSS-data and has, therefore, been

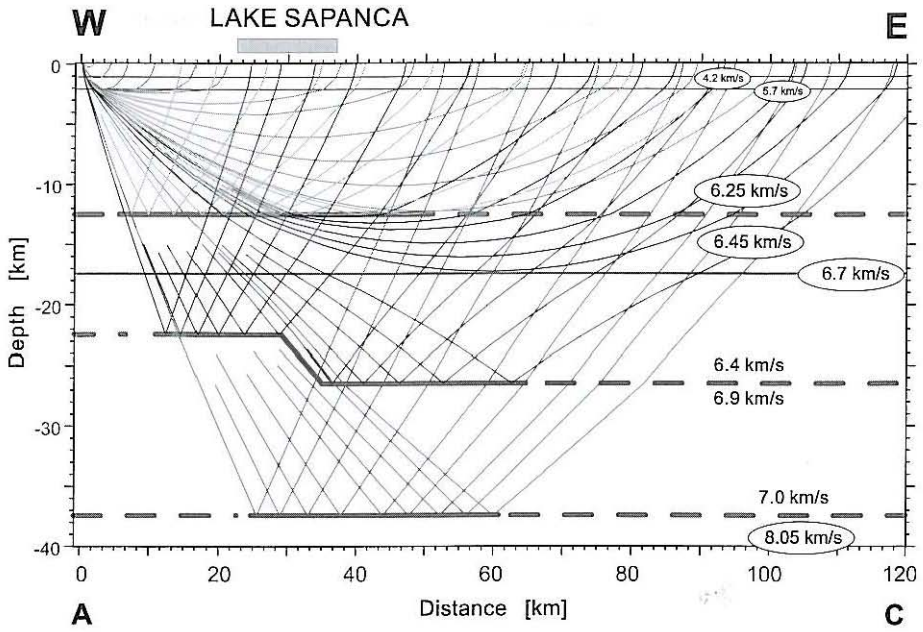

Fig. 4. W-E crustal section, raytracing model of the crust (rays for Shotpoint A are shown).

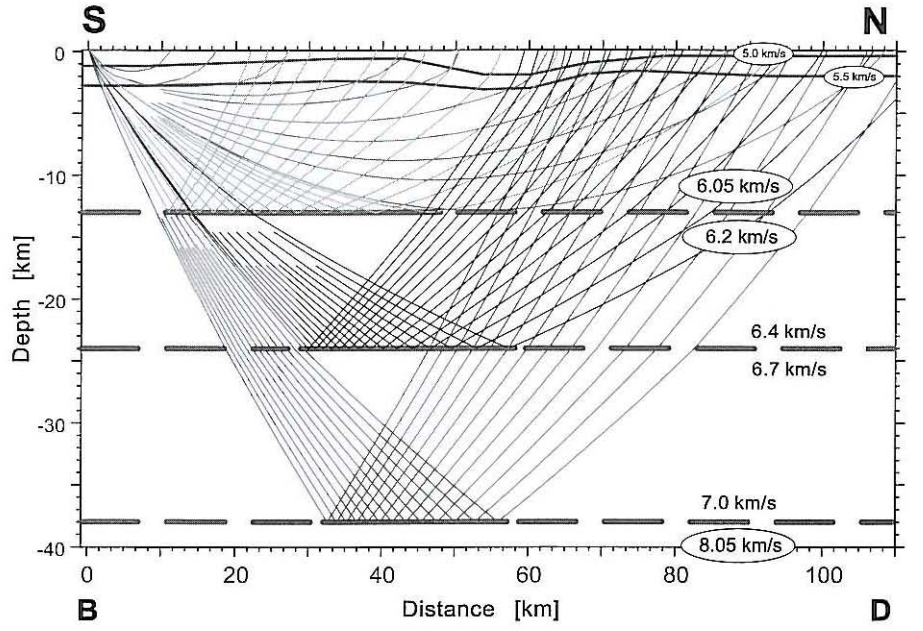

Fig. 5. S-N crustal section, raytracing model of the crust (rays for Shotpoint B are shown).

omitted. $P_M P$ appears at three stations beyond 110 km. This is in reasonable agreement with a Moho depth of 38 km.

Shotpoint E, Profile Section E-A (Akyazi-Izmit) (fig. 3b) – A sediment layer with velocities of 2.25-3.15 km/s delays P_g (V_p = 5.8 km/s) by 0.2 to 0.4 s. This is attributed to a thicker sediment cover in the Akyazi basin. A later arrival marked by open diamonds refers to wide angle reflections from the middle crust.

Shotpoint C, Profile Section C-E (Abant-Akyazi) (fig. 3c) – This profile may be discussed together with fig. 3d.

Shotpoint E, Profile Section E-C (Akyazi-Abant) (fig. 3d) – Between 10 and 50 km first arrivals on the west-east profile C-E (fig. 3c) yield an apparent P_g-velocity of 5.5 km/s while on the reverse profile (fig. 3d) P_g appears with a velocity of 5.9 km/s. This may be due to a dip of the top of the crystalline toward the Akyazi basin having a true velocity of 5.7 km/s. On Profile E-C at larger distances the P_g velocity reaches 6.24 km/s. No clear reflections from the deeper crust have been observed. The profiles traverse metamorphic and volcanic units.

5.2. *N-S Profile (Karasu-Yenipazar)*

Shotpoint D (fig. 3e) – Shotpoint D in the north, near the Black Sea, apparently produces low frequency signals. With a delay time of 0.6 s the sediment cover is very thin in the north and reaches, as seen on the reverse Profile E-D (fig. 3f), a maximum thickness of 2-3 km in the Akyazi basin. P_g-velocity increases in steps from 5.2 km/s to 5.6 km/s from north to south. A strong slow phase with a velocity of 3.1 km/s at short distances up to about 30 km from D might be S_g if the source is a strong *S*-wave radiator.

Reflections from the upper crust, as seen on the E-W Profile, cannot be correlated.

Shotpoint E, Profile Section E-D (fig. 3f) – Near to the shotpoint a sediment thickness of 2-3 km delays P_g by about 1s.

The apparent P_g velocity of 5.82 km/s on the reverse Profile Section E-D is in agreement with a northward thinning of the sedimentary cover. Between 20 and 50 km late arrivals with t_{red} of 1.8-2.2 s may represent wide angle reflections from the upper crust.

Shotpoint B (fig. 3g) – B is the southernmost shotpoint in the Mesozoic Karadag block. To the first 10 km of the Profile B-D an apparent velocity of 3.9 km/s can be attributed, which is faster than the sediment velocity on previous profiles. The thickness of this sediment layer is calculated to be about 1 km. A P_g-velocity of 5.7-5.9 km/s is found along the entire profile. Between 70 and 100 km, $P_M P$ (star symbols) can be traced quite well and provide important evidence for a Moho depth of 38 km. From the mean of several raytracing tests Karahan (1998) concluded that this value is comparatively stable. An uncertainty of the Moho depth of ± 2 km may be admissible (see also Section 5.4).

A ray tracing model for the data of Profile B-D is shown in fig. 5

5.3. *The Imroz earthquake*

As previously mentioned, an M_b ~ 4.5 earthquake occurred on 12 October 1991, T_0 = 16:32:37.5 UT at 40.2°N 26.65°E and h = 8 ± 6 km. At this time the Profile Section A-E was occupied by 30 recording stations. In addition, data from about 20 permanent earthquake stations of the Mudurnu- and MARNET-networks (fig. 6) were available. The evaluation of the first arrivals permitted a very accurate P_n velocity determination of 8.05 km/s below the test area (fig. 7). Of particular interest is a travel time delay of about 0.8 s at an epicentral distance of about 360 km. Using the available information from DSS, it has been verified that this delay cannot be explained only by the variations in thickness of the sediments. The offset can best be explained by a step of the crust-mantle boundary of approximately 14 km about 40 km east of Shotpoint A. A ray tracing model is shown in fig. 8. It may be suggested that this step is related to that found in the lower crust on refraction Profile A-C (fig. 4). In this way the Imroz earthquake contributed to our DSS experiment in two important ways.

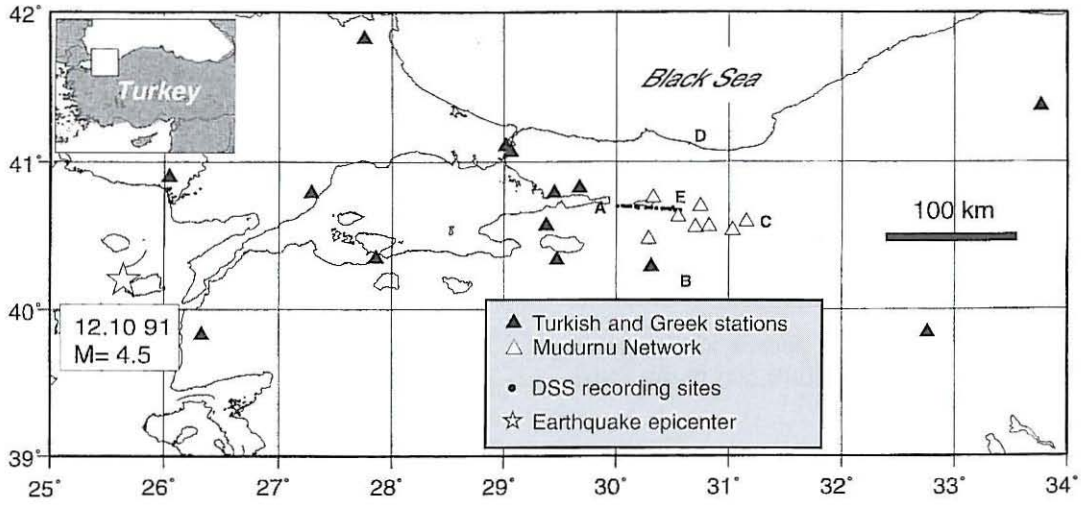

Fig. 6. Imroz earthquake of October 12, 1991: epicenter and position of recording stations.

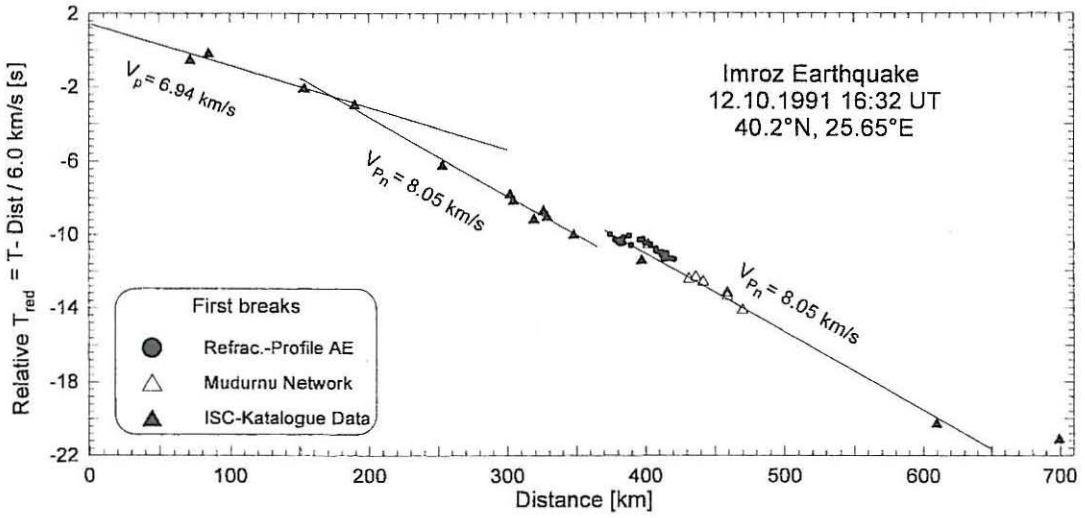

Fig. 7. Imroz earthquake: times of first arrivals, reduced by 6.0 km/s.

5.4. *The average or generalized crustal model*

As mentioned in the introduction, a major aim of the deep seismic sounding experiment was to obtain a reliable *P*-wave crustal model, representative of the test area, in order to allow a more precise hypocenter determination of local earthquakes. This generalised model should be based on the main information from all profiles, neglecting particular local differences.

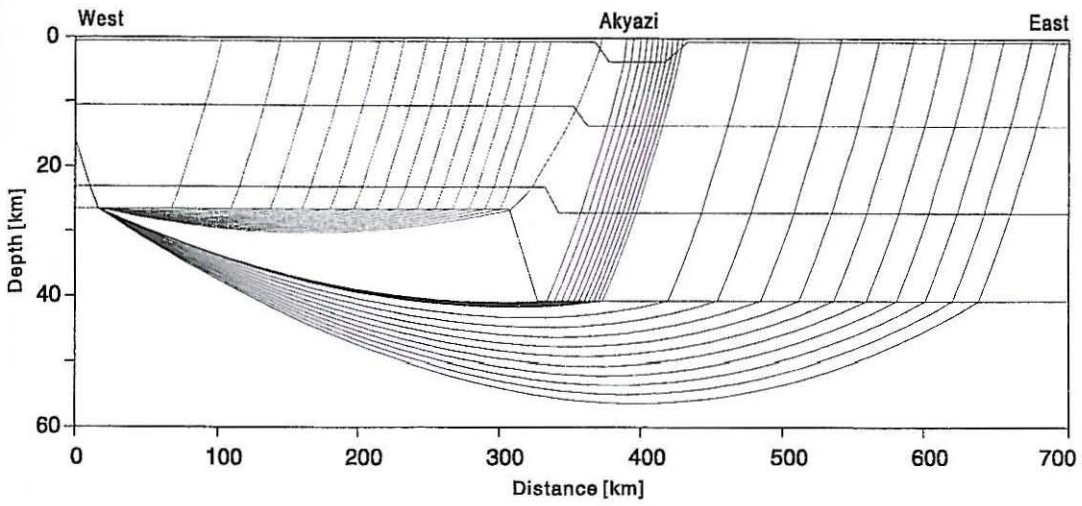

Fig. 8. Raytracing model based on Imroz earthquake travel times and DSS-data.

Therefore, all the arrival times picked in the seismogram sections fig. 3a-h were compiled in fig. 9 and correlated by a few averaging travel time curves. It is seen that the branches of P_g and $P_M P$ are developed quite well. In addition, strong refraction first arrivals and some reflections from the middle crust are also significant. However, P_n is not seen as first arrival due to the limitation in length of the profiles as mentioned in Section 2. Thus, most of the information on the lower crust and the Moho is derived from wide angle reflections $P_M P$ and those from reflectors in the crust. Supplementary information, in particular on the P_n-velocity was provided by the Imroz earthquake (see Section 5.3). By raytracing inversion of the data of fig. 9 and restriction to horizontal layering, a crustal model with velocity gradients was achieved and is shown in fig. 10 (solid line). Below a thin (2 km) sediment layer with average velocity of about 2 km/s, the crystalline basement is reached, where the velocity increases from 5.65 km/s to 6.6 km/s at 15 km depth. This is followed by a zone with negative velocity gradient down to 24 km. These layers compose the upper and middle crust. The lower crust has an average velocity of 7.0 km/s and reaches the Moho at a depth of 39 km, where the velocity rises to 8.05 km/s. From this model, an almost equivalent model with constant layer velocities (dashed lines in fig. 10) can be deduced. This is particularly suitable for direct application *e.g.* in the HYPO 71 – focal locating program.

To test the stability of the generalised gradient model, parameters of velocities and layer thicknesses were modified in the different depth ranges of the crust (upper, middle, lower crust) by ± 0.2 km/s in velocities and ± 2 km in the layer thicknesses. For details see Karahan (1998). It may be stated that parameter modifications as indicated above cause in most cases considerable inconsistencies with the data, in particular:

– Travel times of P_g vary more with change in velocity than with layer thickness.

– Travel time of the reflection from 13 km depth is sensitive to perturbations of both, velocity and depth of the discontinuity.

– Travel time of the diving wave from 17 km depth reacts sensitively to variations of velocity of the middle crust but not to those in depth of the discontinuity.

– Travel time of the reflection from the 24 km discontinuity reacts significantly to alterations of velocity and of depth.

– The travel time of the Moho reflection is only weakly influenced by modifications of the

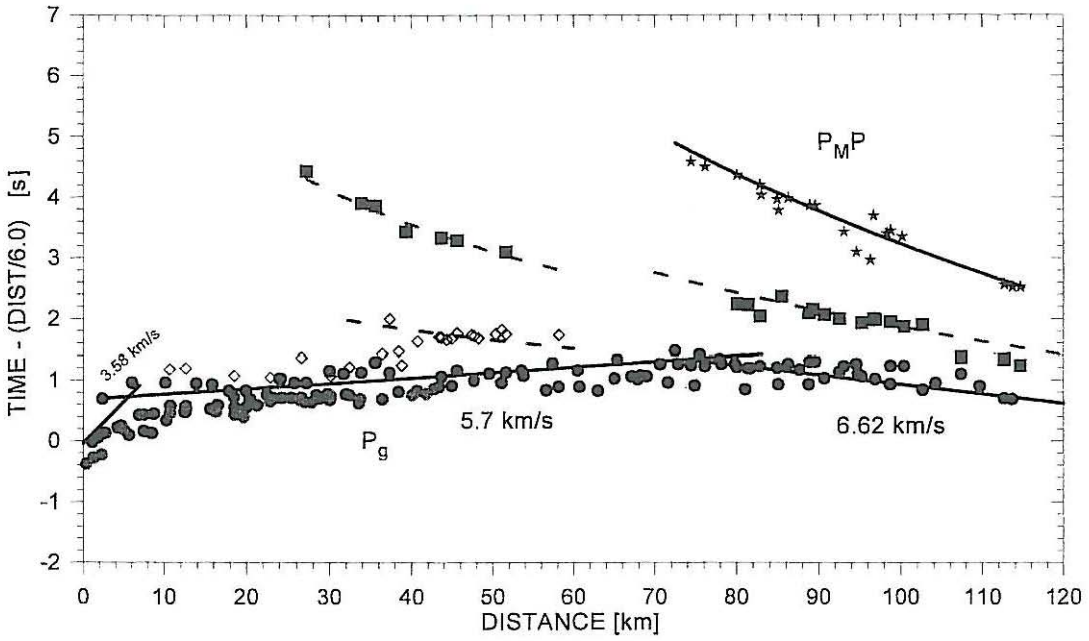

Fig. 9. Compilation of first and later arrivals from Shotpoints A, B, C, D reduced to a common reference level of 100 m NN. Symbols are as in fig. 3a-h, lower part.

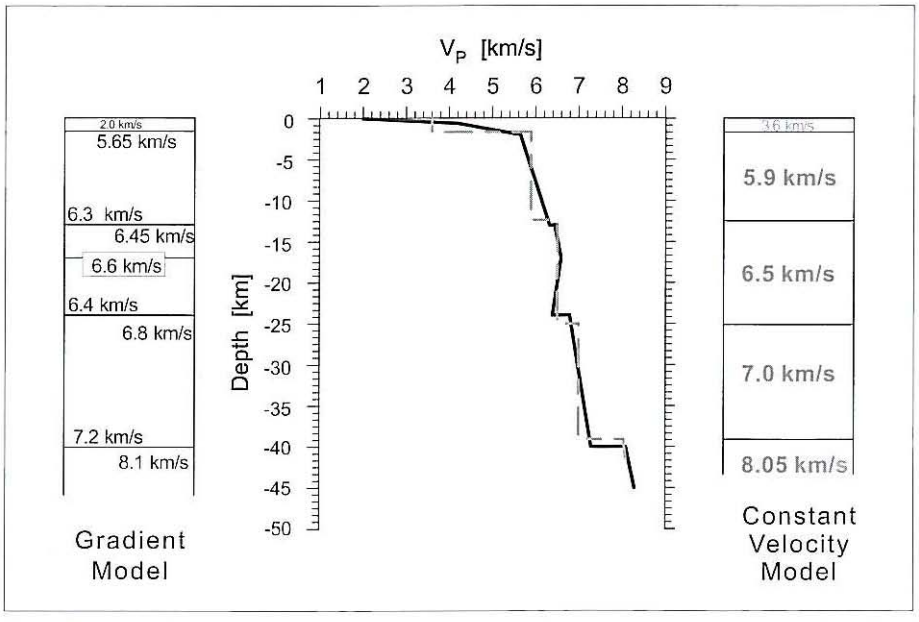

Fig. 10. Generalized crustal models: gradient model (solid line); constant velocity model (dashed line).

velocity in the lower crust but responds more strongly to variation of the Moho-depth. This means that the calculation of the Moho depth is comparatively reliable.

6. Discussion of the results

The generalized crustal model derived from the composed data of the two orthogonal profiles is a rather stable solution of the travel time inversion and may be considered as representative for Northwestern Anatolia.

In detail, four semi-profiles with shotpoint E at the center, differ in the first place by their initial velocities and intercept times of the crystalline phase. At Shotpoint E, in northern and western directions, P_g is delayed. This is due to differences in the sediment cover. In the splitting zone of the branches of the NAFZ (see fig. 1) a holocene pull-apart basin near Akyazi or a fault overstep (Neugebauer *et al.*, 1997) may have developed. The second arrivals with $t_{red} \approx 2$ s west of Shotpoint A have been interpreted as side wall reflections from the Paleozoic Sakarya block bordering the Izmit-Sapanca-trough in the south.

It is found that in the second half of the Profiles E-C and C-E, there are no reflections from the middle crust at about 13 km depth. However, those are observed on the other profiles well.

On the long Profiles A-C, B-D and D-B at shotpoint distances above 80 km reflections with t_{red} 1.0-2.0 s are observed, representing reflectors at a depth of about 25 km. In addition, near Lake Sapanca, the Profile A-C shows a significant step in the refractor depth from 22 km to 26 km. A similar or even more pronounced step may exist in the Moho in the same region. This is indicated in the P_n travel time data from the Imroz earthquake (Section 5.3). In this case, the Westernmost Anatolia would rest on a high block of the crust while most of the profiles are on a lower block of the Anatolian crust. This would qualitatively explain some of the inconsistencies with the data of Gürbüz *et al.* (1980), who found a crustal thickness of only 27-29 km. Due to the limitation in the permitted charge size the profile length was restricted to 120 km. Information on the Moho depth is taken from wide angle reflections, some of which are very good quality.

Addendum

During the preparation of this paper two catastrophic earthquakes occurred in the region under investigation. The first one on 17 August 1999 with $M_W \approx 7.4$ destroyed large parts of the city of Izmit, and caused severe damage between Yalova in the west and Düzce in the east. More than 15000 people lost their life. The earthquake occurred after 30 years of quiescence at the western end of the well known sequence of major earthquakes along the North Anatolian Fault (NAF) beginning in 1939.

A second earthquake on 12 November 1999 with $M_W \approx 7.1$ destroyed large parts of Düzce and Adapazari and killed about 1000 people.

The seismic crustal model described in this paper may be of particular interest, and has already been used, for a more precise locating of aftershocks in this region.

In view of the possible cause of the Izmit earthquake finding a significant step in refractor depth in the crust near Lake Sapanca as described in Section 5.1 appears in a new light. There are two different possibilities to explain this discontinuity in structure. Either it is a vertical step in essentially the same type of crust, or the seismic profile traverses the boundary between adjacent blocks of different crustal type, the Pontides in the north and the Anatolides in the south. In any case it represents a large scale heterogeneity of the crustal structure which is frequently also a heterogeneity in strength and stress. After Das and Aki (1977), regions of high strength are called barriers. With reference to our paper (Neugebauer *et al.*, 1997) we prefer the interpretation as a *stepover*, or in terms of dislocation mechanics, as a *jog* in the North Anatolian Fault between NAF1 and the more eastern fracture zone of the 1969 Mudurnu earthquake with a horizontal offset of some 20 km. There were differing opinions about the significance of NAF1 and NAF2 (fig. 1) being the active western continuation of the NAF. The

Izmit-earthquake, but also the micro earthquake activity in previous years, have proven that NAF1 has to be considered the active branch of the NAF. According to Barka and Kadinsky-Cade (1988), and Scholz (1990) large scale jogs present impediments to rupture and, in extreme cases, rupture termination. So it may have needed accumulation of large stress and, consequently, a long time to break that barrier. From model calculations Stein *et al.* (1997) also found a significant stress concentration in that region and identified it as a zone of high potential for a major earthquake. Also the observation by Westerhaus *et al.* (1997) of anomalously high *b*-values in the magnitude-frequency distribution of that region fit into the picture of high heterogeneity and plastic deformation at this corner of the jog.

Because of the extreme danger for the Istanbul region it is suggested to extend the deep seismic sounding investigation in this area to a three dimensional survey.

Acknowledgements

The authors wish to thank all the participants in the field work for their commitment.

Valuable help – explosives as well as drilling – and shooting equipment – came from TPAO (Turkish Petroleum Company). Administrative aid was given by various Turkish regional and local authorities.

Thanks are also expressed to all the private persons, who gave permission to set recording stations on their ground, and to local authorities for providing land for shotpoints.

The experiment was part of the German-Turkish-Research-Project for earthquake prediction research and was carried out under the guidance of the Institute for Meteorology and Geophysics, University of Frankfurt/Germany and the Earthquake Research Institute (Deprem Arastirma Dairesi), Ankara. Thanks are also expressed to Dr. Michael James for linguistic improvement of the text. The project was financially supported by the Deutsche Forschungsgemeinschaft under contract Zs 4/4-9.

The careful and critical reading of the manuscript by the referees is kindly acknowledged.

REFERENCES

BARKA, A., K. KADINSKY-CADE (1988): Strike-slip fault geometry in Turkey and its influence on earthquake activity, *Tectonics*, **7**, 663-684.

DAS, S. and K. AKI (1977): Fault planes with barriers versatile earthquake model, *J. Geophys. Res.*, **82**, 5658-5670.

DEWEY, J.F., M.R. HAMPTON, W.S.F. KIDD, F. SAROGLU and A.M.C. SENGÖR (1986): Shortening of continental lithosphere: the neotectonic of Eastern Anatolia – a young collision zone, in *Collision Tectonics*, edited by M.P. COWARD and A.C. RIES, *Geol. Soc. London, Spec. Publ.*, **19**, 3-36.

GÜRBÜZ, C., S.B. ÜCER and H. ÖZDEMIR (1980): Adapazari yöresinde yapilan patlatma ile ilgili ön degerlendir-me sonuclari (Steinbruch Nähe Adapazari), *Deprem Arastirma Bülteni*, **31**, 73-80.

GÜRBÜZ, C., S. PÜSKÜLCÜ and S.B. ÜCER (1991): A study of crustal structure in the Marmara region using earthquake data, North Anatolian Fault, *Report 4*, 29-41.

KARAHAN, A.E. (1998): *Seismische Tiefsondierung der Krustenstruktur im Mudurnu – Gebiet (NW-Türkei) Diplomarbeit*, Institut für Meteorologie und Geophysik der Universität Frankfurt am Main, pp. 131

KÜLELI, H.S., C. GÜRBÜZ, G. HORASAN and L. GÜLEN (1996): Seismic velocity distribution in the Aegean region, *Eos, Trans. Am. Geophys. Un.*, **77**, 476-477.

NEUGEBAUER, J., M. LÖFFLER, H. BERCKHEMER and A. YATMAN (1997): Seismic observations at an overstep of the Western North Anatolian Fault (Abant-Sapanca region, Turkey), *Geol. Rundsch.*, **86**, 93-102.

SCHOLZ, C.H. (1990): *The Mechanics of Earthquakes and Faulting* (Cambridge University Press), p. 152.

SCHULZE-FRERICHS, K. (1988): Digitale Verarbeitung und Interpretation Weitwinkelseismischer Beobachtungen entlang des Profils DEKORP 2-Süd/Abschnitt Nord, Diplomarbeit, Institut für Meteorologie und Geophysik der Universität Frankfurt am Main.

SENGÖR, A.M.C., N. GÖRÜR and F. SAROGLU (1985): Strike-slip faulting and related basin formation in zones of tectonic escape: Turkey as a case study, in *Strike Slip Deformation, Basin Formation and Sedimentation, Soc. Econ. Paleontol. Mineral. Spec. Publ.*, **37**, 227-264.

STEIN, R.S., A. BARKA and J.H. DIETERICH (1997): Progressive failure on the North Anatolian fault since 1939 by earthquake stress triggering, *Geophys. J. Int.*, **128**, 594-604.

WEBER, M. (1986): Die Gauß-Beams Methode zur Berechnung theoretischer Seismogramme in absorbierenden inhomogenen Medien: Test und Anwendungs-Berichte des Instituts für Meteorologie und Geophysik der Universität Frankfurt am Main, Na-2/66, pp. 141.

WESTERHAUS, M., M. WYSS, R. YILMAZ and J. ZSCHAU (1997): Variations of the *b*-value in space and time and the state of deformation along a junction of the North-Anatolian Fault System, German – Turkish Research Project on the seismoactive zone of the North-Anatolian Fault Zone, German Research Society , *Final Report Part II.*

(received March 23, 2000;
accepted February 26, 2001)